

## Composite Source Mechanism Characterization of Microseismic Data at Pouce Coupe Field, Alberta, Canada

Matthew J Lee (1), Thomas L. Davis (1) and Shawn Maxwell (2)

(1) – Colorado School of Mines, Golden, Colorado

(2) – Schlumberger, Calgary, Alberta

### Summary

The Reservoir Characterization Project at Colorado School of Mines has been working in conjunction with Talisman Energy Inc. since 2009 to analyze two hydraulic stimulations in the Montney Shale play in Canada. Specifically, the project originates from the monitoring of two five stage horizontals from the Pouce Coupe area in North-Western Alberta. The completions were monitored by a variety of microseismic methods (surface, shallow water well and downhole). This paper will focus on analysis of the downhole arrays.

Amplitude ratios of seismic waves (P, Sh and Sv) from groups of events can be used to estimate composite focal mechanism solutions in areas where a full moment tensor inversion is not effective. In this case, due to the limited azimuths available from the two recording arrays, amplitude ratios are seen as a more robust tool to ascertain these mechanism solutions. Amplitude ratios also utilize data that is already available through processing and this work provides an example of additional analysis possible on existing data. A technique is implemented to model the radiation patterns from simple end member mechanisms (pure double-couple or tensile sources) to match the microseismic amplitudes recorded by the downhole arrays. Similar to previous studies in this area, this work finds that the best fit solution is a close to vertical strike-slip mechanism striking at an angle similar to that of maximum horizontal stress (N40E) within the reservoir.

### Introduction

Microseismic monitoring of two hydraulic stimulations within the Montney Formation provides a means to analyze the dominate failure mechanism of microseismic events within the reservoir. The data from two horizontal wells each with five stages located just east of the town of Pouce Coupe in North-Western Alberta are used in this study. The stress regime in the area (Figure 1a) is strike-slip.

The two horizontal wells (Figure 1b), the 2-7 and 7-7, were monitored by two arrays of 3C geophones in nearby monitor wells, the 8-7 and 9-7. The microseismic events were independently processed resulting in four sets of microseismic event locations (Figures 2a, 2b, 2c and 2d). For each of these microseismic events the maximum amplitude of each of the seismic modes (P, Sh and Sv) were recorded and provided to Talisman.

This work uses the amplitude ratios of these seismic waves (Sh/P, Sh/Sv and Sv/P) and compares them to known amplitude radiation patterns for simple seismic sources (strike-slip, dip-slip and tensile failure). Amplitude ratios are convenient, since the ratio is less sensitive to transmission effects. Using three separate amplitude ratios constraints the result and improves the uniqueness leading to an estimate of the strike and dip of the failure related to the microseismic event. By comparing these results with other independent natural fracture determination techniques (shear wave splitting map and

an FMI log), this work supports the theory that the majority of microseismic events we record are shear dominated and a result of failure along existing weak planes.

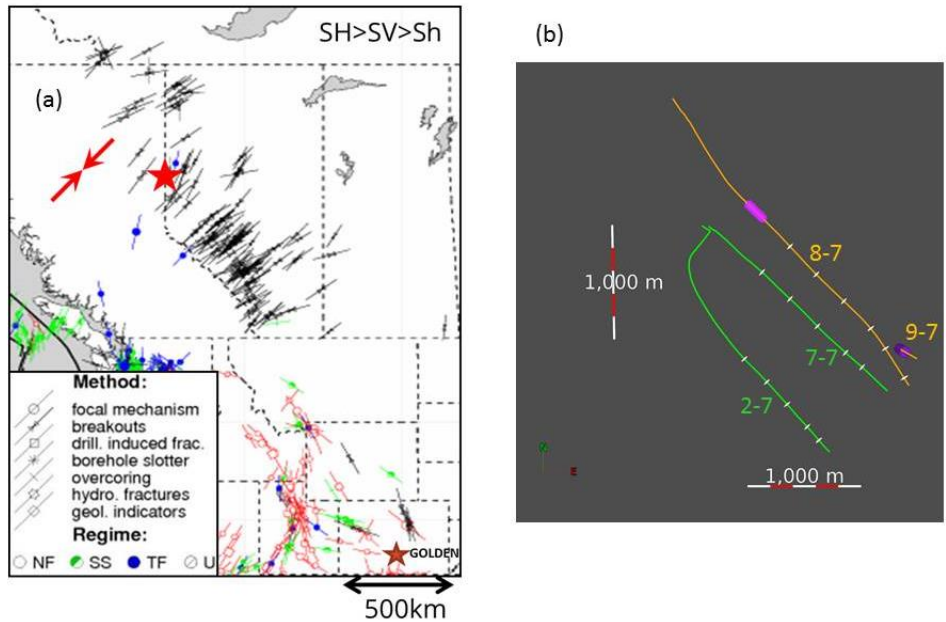


**Figure 1:** (a) The red star shows the approximate location of the study. A series of lines show the direction of maximum horizontal stress in the area. There is a consistent N40°E direction due to the compression of the nearby rocky mountains highlighted by the red arrows. (b) Well layout for this study. The green wells are the two hydraulically stimulated wells with the white dashes showing perforation locations. The 2-7 is completed in the Montney C and the 7-7 is completed in the Montney D. The orange wells are the monitor wells. The 8-7 horizontal contains a ten string array near the heel of the well at the Montney C level (purple) and the 9-7 vertical well has a 50 tool array spanning 735m of vertical depth with only the bottom two sondes located in the Montney interval.

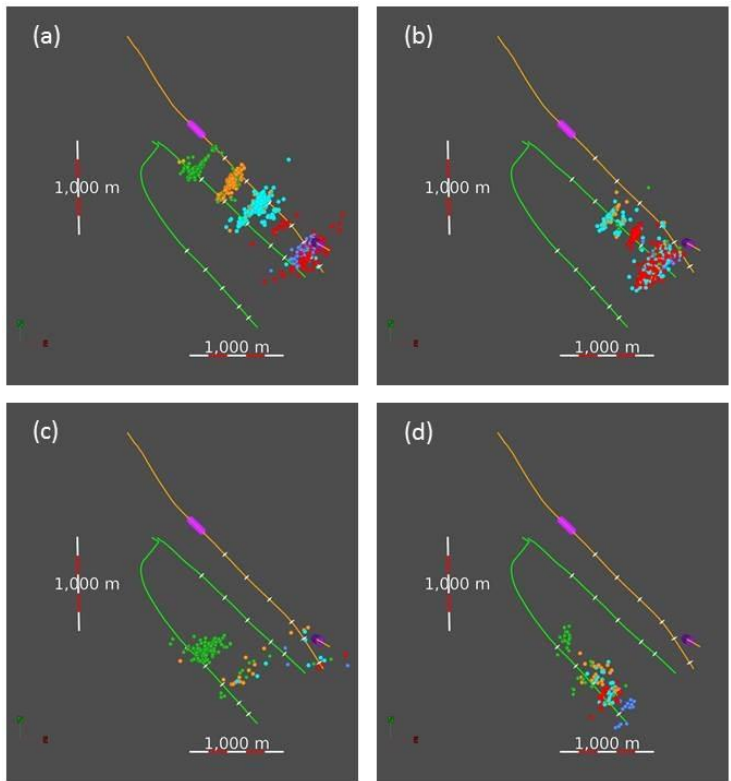


**Figure 2:** Microseismic events for the two horizontal wells. (a) 7-7 well recorded by the 8-7 horizontal array (b) 7-7 well recorded by the 9-7 vertical array (c) 2-7 well recorded by the 8-7 horizontal array (d) 2-7 well recorded by the 9-7 vertical array. For each of the figures stage 1 is in blue, stage 2 red, stage 3 light blue, stage 4 orange and stage 5 green. In general the quality of the microseismic data is good and the recorded amplitudes are consistent. There are some issues with event locations in (c) which leads to only the stage 5 events being used in the amplitude ratio analysis. Stages are occasionally co-located such as stages 1 and 2 in (a) and stages 2 and 3 in (d). In such cases similar failure mechanisms are found and only one solution is given. Stages 3, 4 and 5 in (b) have no amplitude data available so no ratios are calculated in these cases.

## Method and Results

Using theoretical radiation patterns of different source types (e.g. Shi and Ben-Zion (2009)); three separate cases are set-up to identify the best fitting mechanism for the microseismic amplitude data. This work focuses on a strike-slip mechanism, a pure dip-slip mechanism, and a tensile failure. Amplitude variations in the far field based on azimuth from source to array and the inclination between event and recording array are calculated for each of these cases.

To filter the available amplitude data, there is some post-processing work done to remove those with limited results and provide a measure of uncertainty to the amplitude ratios. Firstly, a measure is imposed that for the events recorded by the 8-7 array, amplitude ratios must be available (i.e. both necessary seismic amplitudes recorded) for all 10 of the sondes. Similarly, at least 15 amplitude ratios must be available from the 50 sonde vertical array in the 9-7 well. This was imposed as it was often only the lower 20 receivers that recorded the microseismic events. Following this the amplitude ratios from all of the sondes were averaged and the standard deviation calculated to provide a sense of the uncertainty in the data point.

Once the amplitude ratios have been processed, they are plotted on a log scale against the azimuth from source to array. Figure 3 shows the Sh/P amplitude data for the three models highlighting that the strike-slip mechanism provides a good fit to the data. Once testing is done on all three amplitude ratios it becomes clear the strike-slip model provides the best fit to the data.

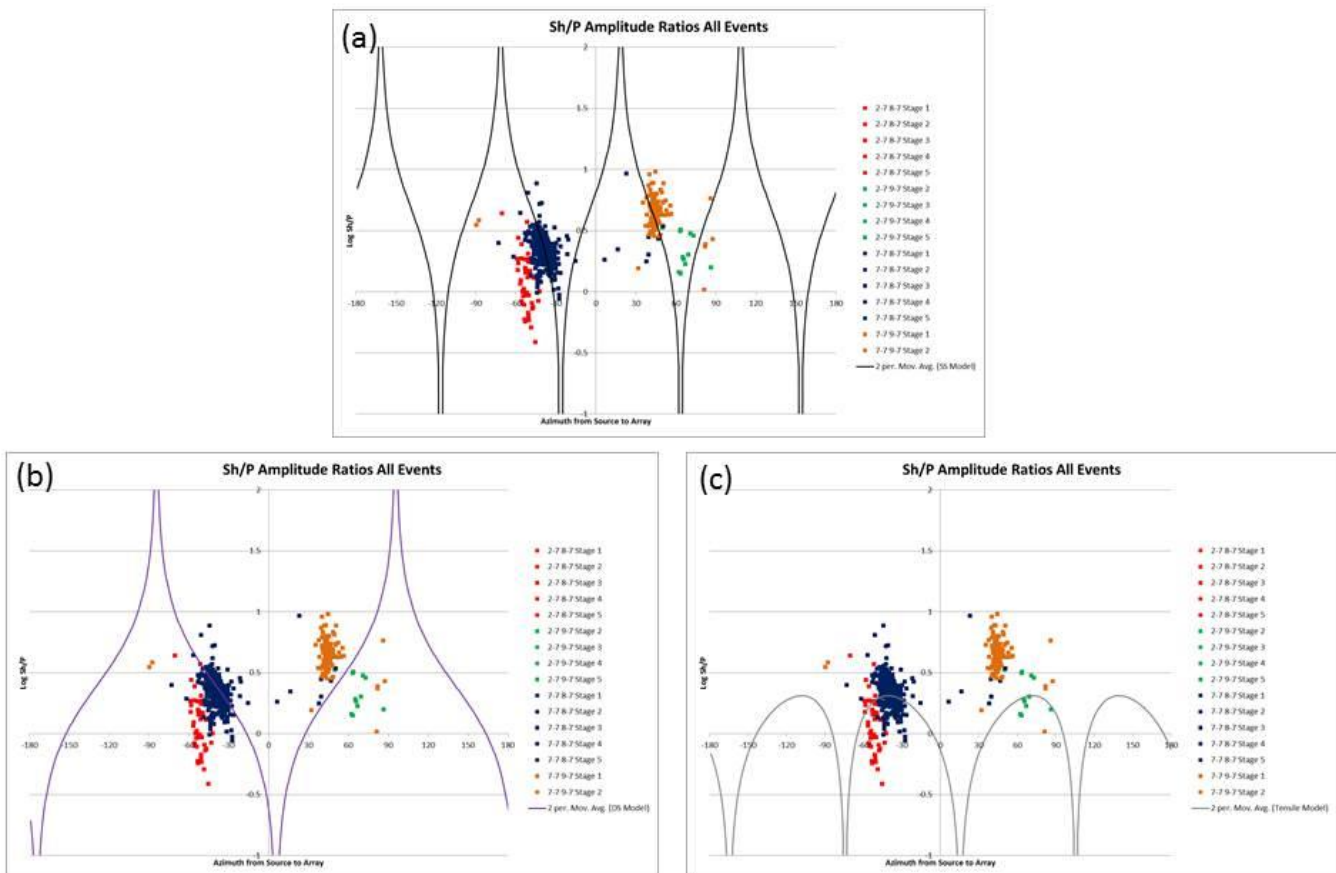


**Figure 3:** Plots for the amplitude data, x-axis is azimuth from source to array and y-axis is the log of the amplitude ratio. Red events are from the 2-7 well recorded by the 8-7, green are 2-7 recorded by the 9-7, blue are 7-7 recorded by the 9-7 and orange are 7-7 recorded by the 9-7. (a) Shows the strike-slip model (b) shows a dip-slip model for a typical inclination between source and array (c) shows a tensile model for the Sh/P data. Only the strike-slip model provides a reasonable fit to all of the data.

It is clear from Figure 3 that the strike-slip mechanism provides the best fit to the data but a single orientation of that mechanism cannot fit all of the results. Therefore each stage on each recording array is plotted individually and a best fit model is drawn for each. The best fit models are based on strike and dip parameters of the strike-slip mechanism. Figure 4 shows the best fit models as fault plane solutions varying across the two completed wells.

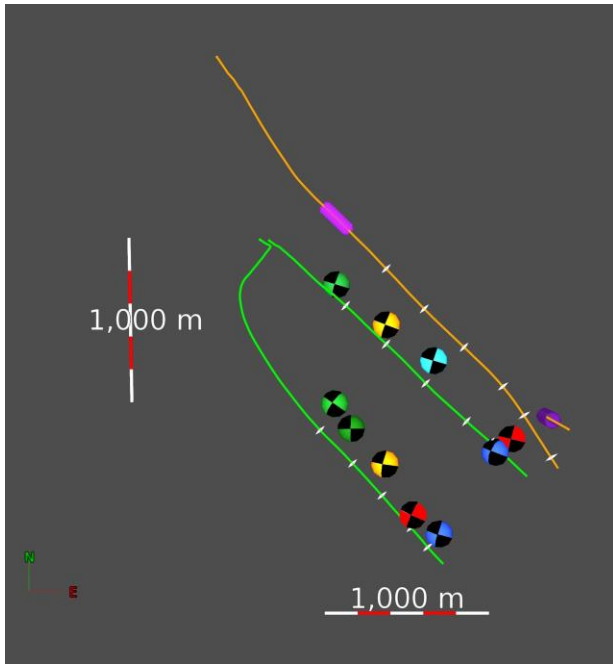


**Figure 4:** Fault plane solutions around the two horizontal wells. In general the solutions are close to 90° dip and their strikes vary from 0-25°. There are two areas where lower dips are seen close to the toe of the 7-7 well and the heel of the 2-7 well. These areas may be related to local wrench fault systems. The strikes of the fault plane solutions are close to the direction of maximum horizontal stress but are not the same angle. This is likely due to different fracture directions within the reservoir. Note that first motion data is not used to solve for sense of slip so regular beach balls are not shown.

Once the solutions were found comparisons were made to other natural fractures determination techniques using the theory that the microseismic events we record are slip along a weak natural plane as a result of an interaction with the propagating hydraulic fracture. Work by Steinhoff (2013) provided a shear wave splitting map of the area. Figure 5 shows the baseline (survey before any hydraulic

fracturing was performed) shear wave splitting map across the area.

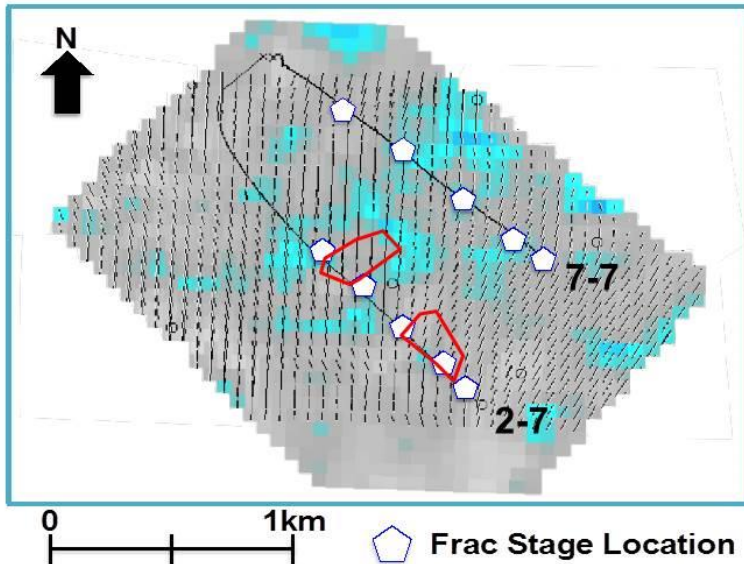


**Figure 5:** Shear wave splitting map of the study area. The dashes in the background are the fast shear directions which provide an estimate of the natural fracture direction. The highlighted areas can be correlated to Figure 4 where the orientation is near north towards the heel of the 2-7 well and rotates to approximately 20° near the toe of the well. Similar correlations between the two methods can be seen across the area.

### Conclusions

The agreement of these two methods supports the theory that microseismic events that we record are slip along natural fractures, explaining why they are often shear dominated and show a large

energy imbalance between what we inject and what we record (Maxwell et al. 2008). The propagating hydraulic fracture which likely holds most of the input energy does not provide a seismic signal which we are capable of recording. Following the completion of these two horizontal wells, an FMI log was ran in the 8-7 horizontal well. Natural fractures identified in this log show similar dips close to 90° and azimuths close to that of maximum horizontal stress (~50-70°). The 8-7 well was later completed in the Montney C and microseismic data from this well are also analyzed. The best fit amplitude ratio solutions show a strike-slip mechanism with similar parameters (strike and dip) to those in the FMI log.

## Acknowledgements

The author would like to thank his committee (Dr. Thomas Davis, Dr. Shawn Maxwell and Dr. Walt Lynn) for their help in creating this work. He also wishes to thank Talisman for supporting the Reservoir Characterization Project and providing this rich data set as well as Pinnacle for returning to their archives to provide the amplitude data necessary to perform this work.

## References

Maxwell, S., Shemetal, J., Campbell, E. and Quirk, D. 2008. *Microseismic Deformation Rate Monitoring*. SPE Annual Technical Conference and Exhibition. SPE116596. pp. 1-9

Shi, Z. and Ben-Zion, Y. 2009. *Seismic radiation from tensile and shear point dislocations between similar and dissimilar solids*. Geophysical Journal International, Vol. 179, pp. 444-458

Steinhoff, C. 2013. *Multicomponent seismic monitoring of the effective stimulated volume associated with hydraulic fracture stimulations in a shale reservoir, Pouce Coupe field, Alberta, Canada*. MS Thesis, Colorado School of Mines